Steel and Composite Structures, *Vol. 27, No. 1 (2018) 1-12*
DOI: https://doi.org/10.12989/scs.2018.27.1.001

Semi-analytical solution of horizontally composite curved I-beam with partial slip

Xu-xi Qin [a], Han-bing Liu [b], Chun-li Wu * and Zheng-wei Gu [c]

College of Traffic, Jilin University, Changchun 130025, P.R. China

(*Received March 27, 2017, Revised July 15, 2017, Accepted August 04, 2017*)

Abstract. This paper presents a semi-analytical solution of simply supported horizontally composite curved I-beam by trigonometric series. The flexibility of the interlayer connectors between layers both in the tangential direction and in the radial direction is taken into account in the proposed formulation. The governing differential equations and the boundary conditions are established by applying the variational approach, which are solved by applying the Fourier series expansion method. The accuracy and efficiency of the proposed formulation are validated by comparing its results with both experimental results reported in the literature and FEM results.

Keywords: curved I-beam; composite beam; slip; variational approach

1. Introduction

In recent years, the composite curved-beam of different materials is often used in bridge structures such as horizontally composite curved steel-concrete bridge. The composite curved-beam shows very complex structural behaviour since the coupling effect of axial, flexural and torsional deformation. In addition, the shear connectors generally permit the development of only partial composite action between the individual components of the member, and their analysis requires the consideration of the interlayer slip between the subcomponents. Therefore, the evaluation of the structural response is of fundamental importance in the design of the composite curved structures.

One of the early work dealing with the stability behaviors of curved beam is the one by Vlasov (1961). After that, many researchers developed different extensions and enhancements to the Vlasov model (Wilson *et al*. 1999, Kim *et al*. 2005a, b, Gimena *et al*. 2008, Kim 2009, Yu *et al*. 2011, Prokic *et al*. 2014, Liu *et al*. 2016, Arefi and Zenkour 2017). However, the analysis and correlative research work of horizontally composite curved beams are relative scarce. Most of the early researches were limited to the assumption of the full interaction between the layers. Thevendran *et al*. (1999, 2000) conducted experiments on the steel-concrete composite curved beam to investigate the ultimate load behavior and a three-dimensional finite element model which has been adopted to simulate the available experimental results. Topkaya *et al*. (2004) conducted experimental and numerical studies to establish the performance of composite curved beam bridges during construction. Giussani and Mola (2006) developed an analytical equation for elastic horizontally curved composite beams with the assumption of the full interaction between the steel girder and concrete slab.

On the other hand, the behaviours of composite beam are significantly influenced by the flexibility of the shear connection. A significant amount of researches have been accomplished in regard to the behavior of straight composite beam with partial shear interaction (Girhammar and Gopu 1993, Dall'Asta 2001, Ranzi *et al*. 2003, Liu *et al*. 2005, Zona and Ranzi 2011, Chakrabarti *et al*. 2012, Santos and Silberschmidt 2014). The previous researches laid the foundation for the curved composite beam. Correspondingly, some researchers have focused on the study of curved composite beam with partial shear interaction. Palani and Rajesekan (1992) presented a finite element formulation for static and stability analysis of thin-walled curved beam of open cross section based on the principle of virtual work. Pi *et al*. (2006) developed a total Lagrangian finite element model for the nonlinear inelastic analysis of both composite beams and columns. After that, Erkmen and Bradford (2009) further extended a 3D elastic total Lagrangian formulation for the numerical analysis of curved in-plan composite steel-concrete beams. Tan and Uy (2009) conducted experimental tests which consist of eight composite steel-concrete beams curved in plan under the action of combined flexure and torsion. In their study, the composite steel-concrete beams were tested with eight test specimens, four were designed with full shear connection, and the other four were designed with partial, shear connection. Qin *et al*. (2016) presented a semi-analytical solution of the simply supported horizontally composite curved I-beam by trigonometric series. But only partial interaction in the tangential direction was considered in

∗Corresponding author, Ph.D.,
E-mail: clwu@jlu.edu.cn
[a] Ph.D.,
E-mail: qinxx29@sina.com
[b] Professor,
E-mail: liuhb2014@sina.com
[c] Ph.D.,
E-mail: zhengweigu123@sina.com

ISSN: 1229-9367 (Print), 1598-6233 (Online)

their research. In fact, due to the coupling effect of bending and torsional deformation, the slip between layers of the composite curved-beam not only produces in the tangential direction but also in the radial direction. Previous researches (Tan and Uy 2011, Liu *et al*. 2012) indicated that it is important to consider the partial interaction in the radial direction as well as in the tangential direction.

In the present paper, a semi-analytical solution of the simply support horizontally composite curved I-beam by trigonometric series is developed. The flexibility of the interlayer connectors between layers both in the tangential direction and in the radial direction is taken into account in the proposed formulation. The beam is assumed to be statically determinate with a constant radius of curvature along the longitudinal axis. Governing equations and boundary conditions are obtained by using the Vlasov curved beam's theory and the principle of energy variation principle. In the procedures, to solve the governing equation of the partial interaction composite beam theory, the undermined vertical deflection, torsional deflection and Lagrange multipliers are approximated by Fourier series, respectively. The advantage of this method is that the calculation can be easily handled and suitable for practical design work.

2. Basic assumptions

A horizontally composite curved I-beam is considered as shown in Fig. 1. Following assumptions are adopted:

- The slab and I-girder are linear-elastic with different materials, all cross-sections remain rigid throughout the deformation. The effect of shear deformation, warping deformation, distortion deformation and sli p due to warping are neglected. The slab and I-girder have the same torsional deflection and vertical deflection.
- The interlayer connectors between the slab and I-girder are continuous. The load-slip behavior of the connectors is described in a linear-elastic range with a constant slip modulus K_t [N/m^2] in the tangential direction and K_t [N/m^2] in the radial direction.
- The frictional effects and uplift between the slab and girder are neglected .The radius of the curvature is a constant along the beam.

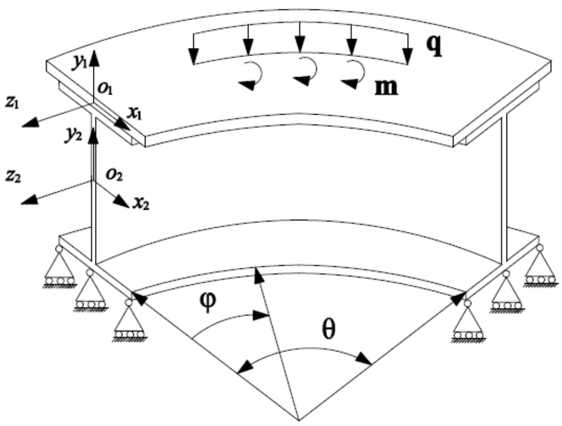

Fig. 1 Model of a horizontally composite curved I-beam

3. Geometry and constitutive relations for each part of the beam

In this paper, the subscripts 'i = 1' and 'i = 2' refer to the slab and I-girder of the cross-section in this paper, respectively. Fig. 2 shows displacement parameters defined at the centroid along the z-axis of the beam. o_i is the centroid on the cross section A_i of the beam. u_{iz}, u_{iy}, u_{ix} and ϕ_{iz}, ϕ_{iy}, ϕ_{ix} are the deflections and rotations of the cross-section in the tangential, vertical direction and radial direction (z-direction, y-direction and x-direction), respectively. According to the basic assumptions, there are

$$\phi_z = \phi_{1z} = \phi_{2z} \tag{1a}$$

$$u_y = u_{1y} = u_{2y} \tag{1b}$$

The components of the displacement vector for an arbitrary point on the thin-walled cross-section can be expressed as follows

$$U_{iz} = u_{iz} - x\phi_{iy} + y\phi_{ix} \tag{2a}$$

$$U_{iy} = u_y + x\phi_z \tag{2b}$$

$$U_{ix} = u_{ix} - y\phi_z \tag{2c}$$

Where $\phi_{iy} = -(u_{ix}' + \frac{u_{iz}}{R})$, $\phi_{ix} = -u_y'$ and $()' = \frac{d()}{dz}$.

According to Eqs. (2a)-(2c), the distributions of strain described in Ref. (Yu *et al*. 2006), on the cross-section, are

$$\sqrt{g}\varepsilon_{iz} = u_z' - yu_y'' + x(u_{ix}'' + \frac{u_{iz}'}{R}) - \frac{1}{R}(u_{ix} - y\phi_z) \tag{3a}$$

$$2\sqrt{g}\gamma_{iyz} = x(\phi_z' + \frac{u_y'}{R}) \tag{3b}$$

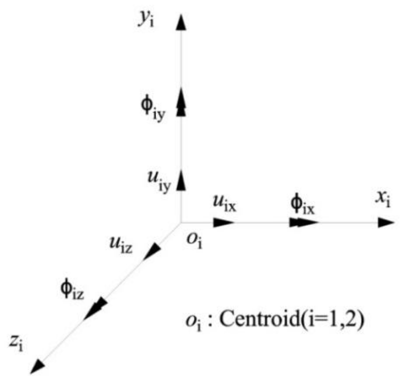

Fig. 2 Displacement parameters of the horizontally composite curved I-beam

$$2\sqrt{g}\gamma_{ixz} = -y(\phi_z' + \frac{u_y'}{R}) \tag{3c}$$

where $()'' = \frac{d^2()}{dz^2}$. R is the radius of the beam. ε_{iz}, γ_{iyz}, γ_{ixz} are the normal strain and shear strain for the slab and I-girder, respectively. Assume that the curvature is small enough to assure that $g = (1-\frac{x}{R})^2 \approx 1$. For the case of isotropic beam under consideration, the stresses can be obtained in terms of the strains as

$$\begin{Bmatrix} \sigma_{iz} \\ \tau_{ixz} \\ \tau_{iyz} \end{Bmatrix} = \begin{bmatrix} E_i & 0 & 0 \\ 0 & G_i & 0 \\ 0 & 0 & G_i \end{bmatrix} \begin{Bmatrix} \varepsilon_{iz} \\ 2\gamma_{ixz} \\ 2\gamma_{iyz} \end{Bmatrix} \tag{4}$$

where σ_{iz}, τ_{ixz}, τ_{iyz} are the normal stress and shear stress for the slab and I-girder, respectively. E_i, G_i are the elasticity modulus and shear modulus, respectively.

According to the relation between the internal forces and stress, the internal forces are defined by

$$N_i = \iint \sigma_{iz} dxdy \tag{5a}$$

$$Q_{ix} = \iint \tau_{ixz} dxdy \tag{5b}$$

$$Q_{iy} = \iint \tau_{iyz} dxdy \tag{5c}$$

$$M_{iz} = \iint (\tau_{iyz} \cdot x - \tau_{ixz} \cdot y) dxdy \tag{5d}$$

$$M_{ix} = -\iint \sigma_{iz} \cdot y dxdy \tag{5e}$$

$$M_{iy} = \iint \sigma_{iz} \cdot x dxdy \tag{5f}$$

where N_i is the axial force, Q_{ix} and Q_{iy} are shear forces, M_{iz} is torque, M_{ix} and M_{iy} are bending moments.

Substituting Eqs. (3) and (4) into Eqs. (5a)-(5f) and

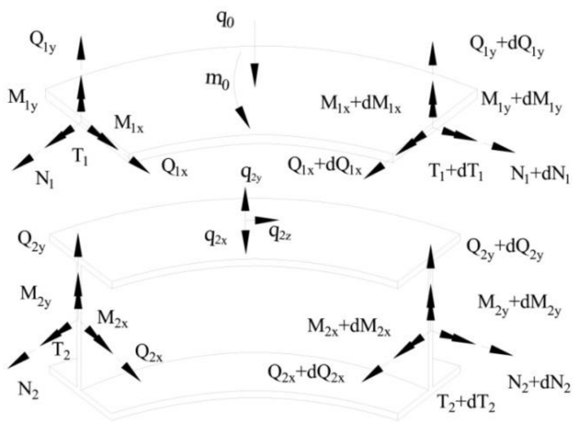

Fig. 3 Force diagram for a micro unit of the horizontally composite curved I-beam

integrating over the cross-section yield the following relations between the force and deformation.

$$\begin{Bmatrix} N_i \\ M_{iy} \\ M_{ix} \\ M_{iz} \end{Bmatrix} = \begin{bmatrix} E_i A_i & 0 & 0 & 0 \\ 0 & E_i I_{iy} & 0 & 0 \\ 0 & 0 & E_i I_{ix} & 0 \\ 0 & 0 & 0 & G_i I_{iz} \end{bmatrix} \begin{Bmatrix} u_{iz}' - \frac{u_{ix}}{R} \\ u_{ix}'' + \frac{u_{iz}'}{R} \\ u_y'' - \frac{\phi_z}{R} \\ \phi_z' + \frac{u_y'}{R} \end{Bmatrix} \tag{6}$$

where A_i, I_{iy}, I_{ix} and I_{iz} are the cross-section area, the second moment of inertia about y, x and z axes, respectively.

4. Equilibrium equations for each part of the beam

Simplifying stress vectors to the centroid O_i on the cross section A_i, as shown in Fig. 3. The external forces and moments per unit length along the axis of the beam are indicated by q_0 and m_0.

The equilibrium equations are

$$\frac{d}{dz}\{Q_i\} - [K]\{Q_i\} + \{q_i\} = \{0\} \tag{7}$$

$$\frac{d}{dz}\{M_i\} - [K]\{M_i\} - [H]\{Q_i\} + \{m_i\} = \{0\} \tag{8}$$

where

$$\{Q_i\} = [N_i, Q_{ix}, Q_{iy}]^T, \quad \{M_i\} = [M_{iz}, M_{ix}, M_{iy}]^T,$$

$$[K] = \begin{bmatrix} 0 & \frac{-1}{R} & 0 \\ \frac{1}{R} & 0 & 0 \\ 0 & 0 & 0 \end{bmatrix}, \quad [H] = \begin{bmatrix} 0 & 0 & 0 \\ 0 & 0 & -1 \\ 0 & 1 & 0 \end{bmatrix},$$

$$\{q_1\} = [q_{1z}, q_{1x}, q_{1y} - q_0]^T, \quad \{q_2\} = [q_{2z}, q_{2x}, q_{2y}]^T,$$

$$\{m_1\} = [m_{1z} + m_0, m_{1x}, 0]^T, \quad \{m_2\} = [m_{2z}, m_{2x}, 0]^T$$

Where m_{ix} is the distributed bending moment produced by shear force q_{iz}, and m_{iz} is distributed torque produced by shear force q_{ix}. For the q_{iz}, q_{ix} and q_{iy}, there are

$$q_{1z} + q_{2z} = 0 \tag{9a}$$

$$q_{1x} + q_{2x} = 0 \tag{9b}$$

$$q_{1y} + q_{2y} = 0 \tag{9c}$$

The Eqs. (7) and (8) which lead to

$$\frac{d}{dz}\{Q_1 + Q_2\} - [K]\{Q_1 + Q_2\} + \{q_1 + q_2\} = \{0\} \tag{10a}$$

$$\frac{d}{dz}\{M_1+M_2\}-[K]\{M_1+M_2\}$$
$$-[H]\{Q_1+Q_2\}+\{m_1+m_2\}=\{0\} \tag{10b}$$

Using Eqs. (9a)-(9c), by eliminating (Q_{1x} + Q_{2x}) from Eqs. (10a) and (10b), we obtain

$$-(M_{1y}+M_{2y})''+\frac{(N_1+N_2)}{R}=0 \tag{11a}$$

$$(N_1+N_2)'+\frac{(M_{1y}+M_{2y})'}{R}=0 \tag{11b}$$

When the beam under vertical load q_0 and torque m_0 only, we can get

$$N_1=-N_2, \tag{12a}$$

$$M_{1y}=-M_{2y} \tag{12b}$$

5. Equilibrium equations at the interface

Considering the Eqs. (7) and (8) and deformations in Fig. 4, the force q_{1z} between the slab and girder can be written as

$$q_{1z}=K_t\Delta u_z=K_t(u_{2z}-u_{1z}+\kappa_x b)$$
$$=-N_1'-\frac{M_{1y}'}{R}=N_2'+\frac{M_{2y}'}{R} \tag{13}$$

Where b = b_1 + b_2, κ_x = u'_y. So the equilibrium at the interface in the tangential direction can be written as

$$u_{2z}'-u_{1z}'+u_y''b+\frac{1}{K_t}(N_1''+\frac{M_{1y}''}{R})=0 \tag{14}$$

Considering the Eqs. (7) and (8) and deformations which are shown in Fig. 5, the force q_{1x} between the slab and girder can be written as

$$q_{1x}=K_r\Delta u_x=K_r(u_{2x}-u_{1x}+\kappa_z b)$$
$$=M_{1y}''-\frac{N_1}{R}=-M_{2y}''+\frac{N_2}{R} \tag{15}$$

Where κ_z = ϕ_z. So the equilibrium at the interface in the radial direction can be written as

$$u_{2x}-u_{1x}+\phi_z b-\frac{1}{K_r}(M_{1y}''-\frac{N_1}{R})=0 \tag{16}$$

Using the Eqs. (6), (14) and (16), by eliminating u'_{2z} from Eq. (14) and u_{2x} from Eq. (16), One can rearrange Eqs. (14) and (16) (equilibriums at the interface) as follows

$$\frac{1}{K_t}(N_1''+\frac{M_{1y}''}{R})+\frac{1}{RK_r}(M_{1y}''-\frac{N_1}{R})$$
$$-S_A N_1-\frac{\phi_z b}{R}+u_y''b=0 \tag{17a}$$

$$\frac{1}{RK_t}(N_1''+\frac{M_{1y}''}{R})-\frac{1}{K_r}(M_{1y}''''-\frac{N_1''}{R})$$
$$-S_y M_{1y}+\frac{u_y''b}{R}+\phi_z''b=0 \tag{17b}$$

Where $S_A=\frac{1}{E_2A_2}+\frac{1}{E_1A_1}$, $S_y=\frac{1}{E_1I_{1y}}+\frac{1}{E_2I_{2y}}$.

6. Problem formulation

The governing differential equations of the beam will be derived through the variational approach. Total potential energy Π^* of the beam takes the form as follows

$$\Pi^*=\Pi_1+\Pi_2+\Pi_K+\lambda_z f_z+\lambda_y f_y-W \tag{18}$$

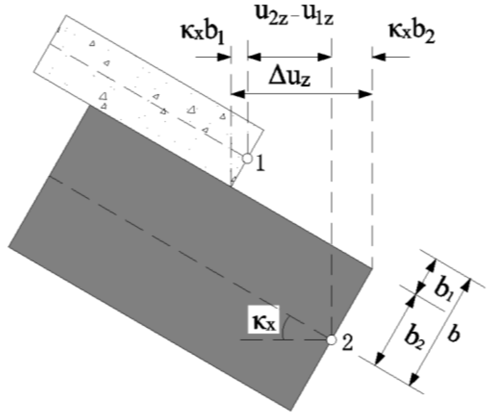

Fig. 4 Deformations of differential elements for the beam in y-z plane

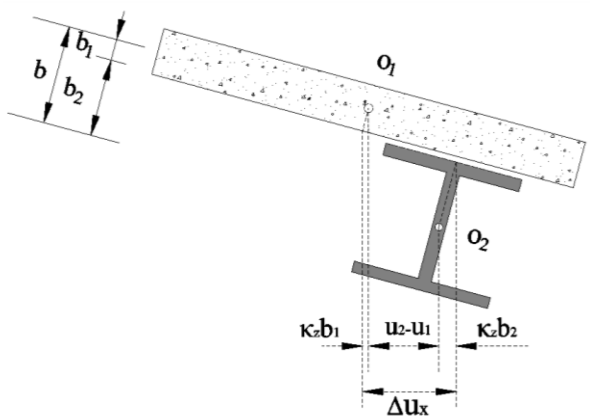

Fig. 5 Deformations for the composite curved I-beam in x-y plane

Where Π_1 and Π_2 are the elastic strain energy of the slab and I-girder, respectively. Π_K is the strain energy due to the connector deformations. W is the potential energy due to the external loading. λ_z, λ_y are the lagrange multipliers. f_z, f_y are the equilibrium conditions at the interface corresponding to Eqs. (17a) and (17b), respectively. These quantities can be expressed as follows

$$\Pi_1 = \frac{1}{2}\int_0^{R\theta} \begin{matrix} [N_1(u_{1z}' - \frac{u_{1x}}{R}) + M_{1z}(\phi_z' + \frac{u_y'}{R}) \\ + M_{1x}(u_y'' - \frac{\phi_z}{R}) + M_{1y}(u_{1x}'' + \frac{u_{1z}'}{R})] \end{matrix} dz \tag{19a}$$

$$\Pi_2 = \frac{1}{2}\int_0^{R\theta} \begin{matrix} [N_2(u_{2z}' - \frac{u_{2x}}{R}) + M_{2z}(\phi_z' + \frac{u_y'}{R}) \\ + M_{2x}(u_y'' - \frac{\phi_z}{R}) + M_{2y}(u_{2x}'' + \frac{u_{2z}'}{R})] \end{matrix} dz \tag{19b}$$

$$\begin{aligned} \Pi_K &= \frac{1}{2}\int_0^{R\theta} (\frac{q_z^2}{K_t} + \frac{q_x^2}{K_r}) dz \\ &= \frac{1}{2}\int_0^{R\theta} [\frac{1}{K_t}(N_1' + \frac{M_{1y}'}{R})^2 + \frac{1}{K_r}(M_{1y}'' - \frac{N_1}{R})^2] dz \end{aligned} \tag{19c}$$

$$\lambda_z f_z = \int_0^{R\theta} \begin{matrix} [\frac{1}{K_t}(N_1'' + \frac{M_{1y}''}{R}) \\ + \frac{1}{RK_r}(M_{1y}'' - \frac{N_1}{R}) - S_A N_1 - \frac{\phi_z b}{R} + u_y'' b]\lambda_z \end{matrix} dz \tag{19d}$$

$$\lambda_y f_y = \int_0^{R\theta} \begin{matrix} [\frac{1}{RK_t}(N_1'' + \frac{M_{1y}''}{R}) \\ - \frac{1}{K_r}(M_{1y}'''' - \frac{N_1''}{R}) - S_y M_{1y} + \frac{u_y'' b}{R} + \phi_z'' b]\lambda_y \end{matrix} dz \tag{19e}$$

$$\begin{aligned} W &= \int_0^{R\theta} m_0 \phi_z dz + \int_0^{R\theta} q_0 u_y dz \\ &+ (M_{xt} u_y')\Big|_0^{R\theta} + (Q_{yt} u_y)\Big|_0^{R\theta} + (T_{zt}\phi_z)\Big|_0^{R\theta} \end{aligned} \tag{19f}$$

where θ is the central angle of the beam. q_z, q_x are the shear force between the slab and girder. There are $q_z = q_{1z}$ and $q_x = q_{1x}$. M_{xt}, Q_{yt}, T_{zt} are the total bending moment, total shear force and total torsion moment of the beam, respectively. ϕ_z, u_y, u_{1x}, u_{1z}, λ_z and λ_y are all unknown variables. The variation of Π^* is

$$\begin{aligned} \delta\Pi^* &= \int_0^{R\theta} \Gamma_1 \delta u_y dz + \int_0^{R\theta} \Gamma_2 \delta\phi_z dz + \int_0^{R\theta} \Gamma_3 \delta\lambda_z dz \\ &+ \int_0^{R\theta} \Gamma_4 \delta\lambda_y dz + \int_0^{R\theta} \Gamma_5 \delta u_{1x} dz + \int_0^{R\theta} \Gamma_6 \delta u_{1z} dz \\ &+ \mathrm{H}_1 \delta u_y\Big|_0^{R\theta} + \mathrm{H}_2 \delta u_y'\Big|_0^{R\theta} + \mathrm{H}_3 \delta\phi_z\Big|_0^{R\theta} + \mathrm{H}_4 \delta\phi_z'\Big|_0^{R\theta} \\ &+ \mathrm{H}_5 \delta[\underbrace{\frac{E_1 I_{y1}}{RK_t}(u_{1x}'' + \frac{u_{1z}'}{R})' + \frac{E_1 A_1}{K_t}(u_{1z}' - \frac{u_{1x}}{R})'}_{\Delta u_z}]\Big|_0^{R\theta} \\ &+ \mathrm{H}_6 \delta[\underbrace{\frac{E_1 I_{y1}}{K_r}(u_{1x}'' + \frac{u_{1z}'}{R})'' - \frac{E_1 A_1}{RK_r}(u_{1z}' - \frac{u_{1x}}{R})}_{\Delta u_x}]\Big|_0^{R\theta} \\ &+ \mathrm{H}_7 \delta[\underbrace{\frac{E_1 I_{y1}}{K_r}(u_{1x}'' + \frac{u_{1z}'}{R})'' - \frac{E_1 A_1}{RK_r}(u_{1z}' - \frac{u_{1x}}{R})]'}_{\Delta u_x'}\Big|_0^{R\theta} \\ &+ \mathrm{H}_8 \delta u_{1z}\Big|_0^{R\theta} + \mathrm{H}_9 \delta u_{1z}'\Big|_0^{R\theta} + \mathrm{H}_{10} \delta u_{1z}''\Big|_0^{R\theta} + \mathrm{H}_{11} \delta u_{1x}\Big|_0^{R\theta} \\ &+ \mathrm{H}_{12} \delta u_{1x}'\Big|_0^{R\theta} + \mathrm{H}_{13} \delta u_{1x}''\Big|_0^{R\theta} + \mathrm{H}_{14} \delta u_{1x}'''\Big|_0^{R\theta} \end{aligned} \tag{20}$$

Where Γ_i (i = 1~6) and H_i (i = 1~14) are calculated from the variation of Π^*, which are given in the Appendix A. By the definition of variational approach, each term for Γ_i (i = 1~6) and H_i (i = 1~14) must be identically zero. When Γ_i (i = 5~6) and H_i (i = 8~14) equal to zero, we can get the undetermined Lagrange multipliers λ_z and λ_y are

$$\begin{aligned} \lambda_z &= E_1 A_1 (u_{1z}' - \frac{u_{1x}}{R}) = N_1 \\ \lambda_y &= E_1 I_{y1} (u_{1x}'' + \frac{u_{1z}'}{R}) = M_{1y} \end{aligned} \tag{21}$$

The Eq. (21) notes that the Lagrange multiplier λ_z equals N_1 (axial force) and Lagrange multiplier λ_y equals M_{1y} (bending moment). It is also can be seen from Eq. (21) that the Lagrange multipliers (λ_z, λ_y) and the deflections (u_{1z}, u_{1x}) are related. Therefore, there'll be four independent variables for the unknown variables. We can take ϕ, w, λ_z and λ_y as independent variables. The rest of governing equations are $\Gamma_i = 0$ (i = 1~4). Which can be rearranged and rendered in terms of matrix form, as follows

$$\begin{bmatrix} EI_x \frac{d^4}{dz^4} - \frac{GI_T}{R^2}\frac{d^2}{dz^2} & -\frac{EI_x + GI_T}{R}\frac{d^2}{dz^2} & b\frac{d^2}{dz^2} & \frac{b}{R}\frac{d^2}{dz^2} \\ -\frac{EI_x + GI_T}{R}\frac{d^2}{dz^2} & -GI_T\frac{d^2}{dz^2} + \frac{EI_x}{R^2} & -\frac{b}{R} & b\frac{d^2}{dz^2} \\ b\frac{d^2}{dz^2} & -\frac{b}{R} & \frac{1}{K_t}\frac{d^2}{dz^2} - \frac{1}{R^2 K_r} - S_A & (\frac{1}{RK_t} + \frac{1}{RK_r})\frac{d^2}{dz^2} \\ \frac{b}{R}\frac{d^2}{dz^2} & b\frac{d^2}{dz^2} & (\frac{1}{RK_t} + \frac{1}{RK_r})\frac{d^2}{dz^2} & -\frac{1}{K_r}\frac{d^4}{dz^4} + \frac{1}{R^2 K_t}\frac{d^2}{dz^2} - S_y \end{bmatrix} \begin{pmatrix} u_y \\ \phi_z \\ \lambda_z \\ \lambda_y \end{pmatrix} = \begin{pmatrix} q_0 \\ m_0 \\ 0 \\ 0 \end{pmatrix} \tag{22}$$

Where $EI_x = E_1 I_{1x} + E_2 I_{2x}$, $GI_T = G_1 I_{1z} + G_2 I_{2z}$. And we can get the pertaining boundary conditions $\mathrm{H}_i = 0$ (i = 1~7).

$$\begin{matrix} [-EI_x(u_y''' - \frac{\phi_z'}{R}) - b\lambda_z' - \frac{b}{R}\lambda_y' \\ + GI_T(\frac{\phi_z'}{R} + \frac{u_y'}{R^2}) - Q_{yt}]\delta u_y \end{matrix}\Bigg|_0^{R\theta} = 0 \tag{23a}$$

$$[EI_x(u_y'' - \frac{\phi_z}{R}) + b\lambda_z + \frac{b}{R}\lambda_y - M_{xt}]\delta u_y'\Big|_0^{R\theta} = 0 \tag{23b}$$

$$[GI_T(\phi_z' + \frac{u_y'}{R}) - b\lambda_y' - T_{zt}]\delta\phi_z \Big|_0^{R\theta} = 0 \tag{23c}$$

$$(b\lambda_y)\delta\phi_z' \Big|_0^{R\theta} = 0 \tag{23d}$$

$$(\lambda_z + \frac{\lambda_y}{R})\delta(\Delta u_z) \Big|_0^{R\theta} = 0 \tag{23e}$$

$$(\lambda_y')\delta(\Delta u_x) \Big|_0^{R\theta} = 0 \tag{23f}$$

$$(-\lambda_y)\delta(\Delta u_x') \Big|_0^{R\theta} = 0 \tag{23g}$$

Where $\Delta u_z = \frac{-1}{K_t}(N_1' + \frac{M_{1y}'}{R})$, $\Delta u_x = \frac{1}{K_r}(M_{1y}'' - \frac{N_1}{R})$.

7. The semi-analytical solution by trigonometric series

The problem can be solved by applying the expansion of Fourier series for a simply supported composite curved I-beam. The independent variables ϕ_z, u_y, λ_z and λ_z can be express as

$$u_y = \sum_{k=1}^{n} u_{yk} \sin(\frac{k\pi z}{L}),$$
$$\phi_z = \sum_{k=1}^{n} \phi_{zk} \sin(\frac{k\pi z}{L}), \tag{24}$$
$$\lambda_z = \sum_{k=1}^{n} \lambda_{zk} \sin(\frac{k\pi z}{L}),$$
$$\lambda_y = \sum_{k=1}^{n} \lambda_{yk} \sin(\frac{k\pi z}{L})$$

Where u_{yk}, ϕ_{zk}, λ_{zk}, λ_{yk} are the unknown Fourier coefficients to be determined for each k (k = 1,…, n). The applied distributed loads q_0 and m_0 are expanded with single trigonometric series as

$$q_0 = \sum_{k=1}^{n} q_{zk} \sin(\frac{k\pi z}{L}),$$
$$m_0 = \sum_{k=1}^{n} m_{zk} \sin(\frac{k\pi z}{L}) \tag{25}$$

Where q_{zk} and m_{zk} are the Fourier coefficients which can be determined by calculus for different load cases, as listed in Table 1. Substituting Eqs. (24) and (25) into the Eq. (22), the unknowns u_{yk}, ϕ_{zk}, λ_{zk}, λ_{yk} can be determined by solving Eq. (22).

8. Numerical examples

To demonstrate the application of this theory and verify the veracity of the semi-analytical method, the results are compared with those available in the literature and with those calculated by finite element analysis.

A FEM (finite element model) proposed by Erkmen (2009) and Majdi (2014) was adopted. In the FEM model shown as in Fig. 6, both the concrete slab and steel I-girder are modeled as 4-node shell elements. The connections

Table 1 The Fourier coefficients for common load cases

Load case	Load diagram	Fourier coefficients for q_{zk} and m_{zk}
1	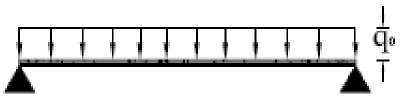	$q_{zk} = \frac{4q_0}{k\pi}$ $(k = 1,3,5...)$
2	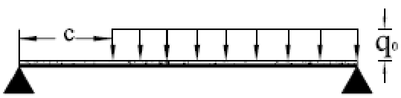	$q_{zk} = \frac{2q_0}{k\pi}[-\cos(k\pi) + \cos(\frac{k\pi c}{l})]$ $(k = 1,2,3...)$
3		$q_{zk} = \frac{2F}{l}\sin(\frac{k\pi c}{l})$ $(k = 1,2,3...)$
4	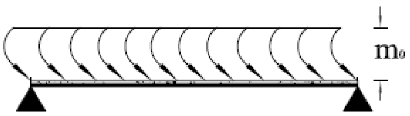	$m_{zk} = \frac{4m_0}{k\pi}$ $(k = 1,3,5...)$
5	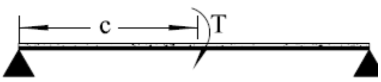	$m_{zk} = \frac{2T}{l}\sin(\frac{k\pi c}{l})$ $(k = 1,2,3...)$
6	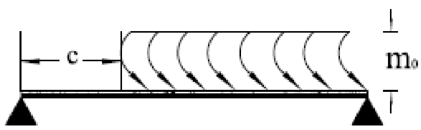	$m_{zk} = \frac{2m_0}{k\pi}[-\cos(k\pi) + \cos(\frac{k\pi c}{l})]$ $(k = 1,2,3...)$

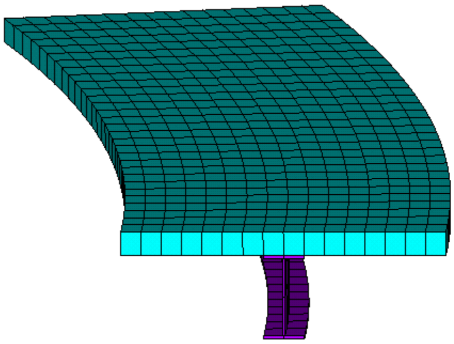

Fig. 6 FEM model of the I-beam

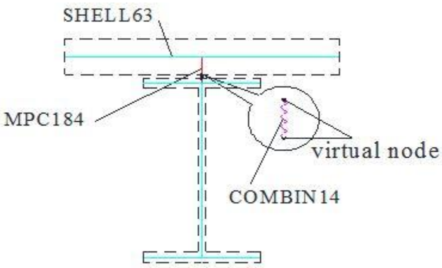

Fig. 7 Connection diagram of the FEM model

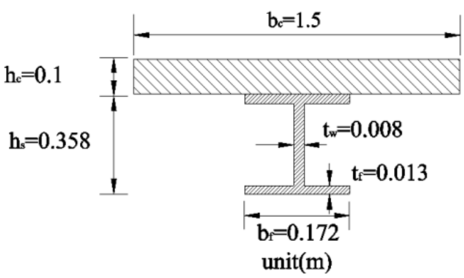

Fig. 8 Cross section dimensions of the curved I-beam

between the slab and I-girder (shown as in Fig. 7) are simulated by multiple-point constraints (MPC), which is modeled by two rigid links connected through nodes between the slab and I-girder. The spring elements are used in the tangential direction and the radial direction to allow for the possibility of movement. Coupling degrees of freedom in vertical direction are used to prevent the uplifting issue.

8.1 Example 1

In this example, a full interaction composite beam with simply supported ends is considered, which has been studied by Thenvendran *et al*. (2000). The beam is subjected to 150 KN, 200 KN and 250 KN vertical loads at the mid-span, respectively. The dimensions of cross section are shown in Fig. 8. Material properties and other dimensions are shown in Table 2. Here, we take 6 terms Fourier series in this case calculation. For the full interaction case, the slip parameter is taken as $K = K_r = K_t = 10^4$ MPa. Fig. 9 shows the vertical deflection results based on the FEM, this paper solution and Thevendran *et al*.'s

Table 2 Material properties and dimensions of the curved I-beam

	Young's modulus (MPa)	Poisson's ratio	Density (kg/m^3)	Central angle	Radius of curvature (m)
Steel girder	E_s = 2.06×10^5	$\mu_s = 0.3$	7850	θ = 14.3°	24
Concrete slab	E_c = 2.6×10^4	$\mu_c = 0.27$	2400		

experimental results. It can be seen that the vertical deflections based on this paper and FEM solutions are in good agreement. The experimental results are also in reasonable agreement with those based on the FEM model and this paper solution as shown in Fig. 9.

8.2 Example 2

To validate the accuracy of present model for the partial interaction, we use the case described by Erkmen (2009). This example also have the same material properties ,geometric properties and loading with example 1 except the shear connector modulus of $K = K_r = K_t = 250$ MPa.

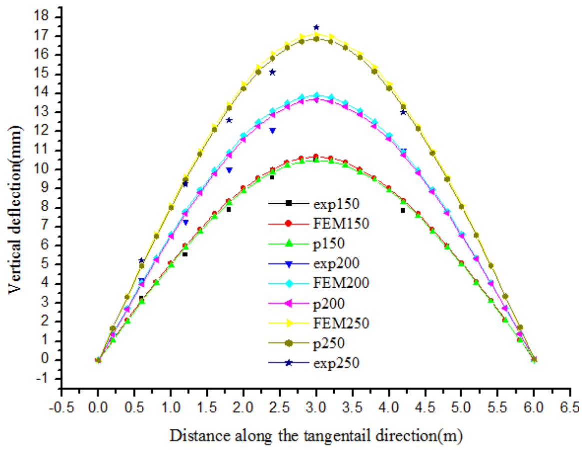

Fig. 9 Torsional angle of the beam with $K = 10^4$ MPa

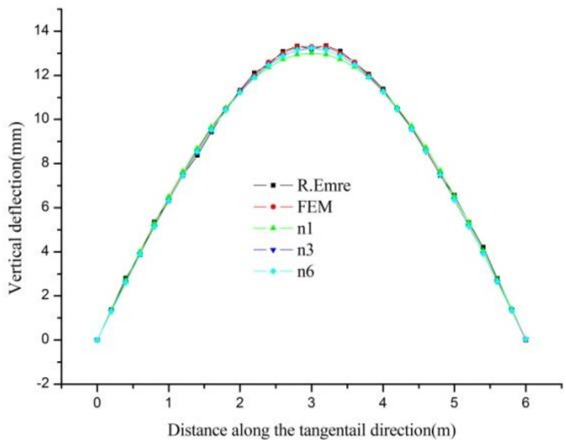

Fig. 10 Vertical deflection of the beam with $K = 250$ MPa

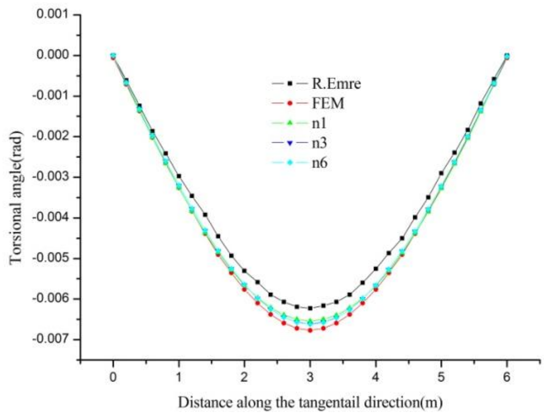

Fig. 11 Torsional angle of the beam with K = 250 MPa

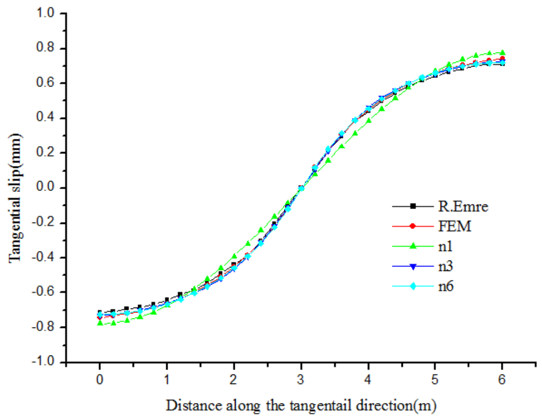

Fig. 12 Tangential slip of the beam with K = 250 MPa

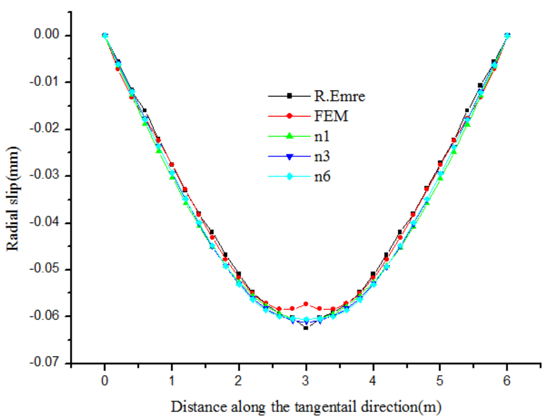

Fig. 13 Radial slip of the beam with K = 250 MPa

Figs. 10-13 show the vertical deflection, torsional angle, tangential slip and radial slip based on the FEM, this paper results and NCE solution by Erkmen (2009), respectively. As an illustration of convergence of the results, we show this paper results by taking 1, 3, and 6 terms of Fourier series respectively. In general, this paper results are in good agreement with NCE and FEM results. The results of numerical calculation show that the method converges very fast, so it is feasible to take the first term or the sum of first three terms only. In order to ensure the accuracy, six terms is adopted in the following example.

8.3 Example 3

In this example, in order to prove the validity of the structure under the load of torque, we examine the load case 4 and 5 shown in Table 1. The model has the same dimensions and other parameters as example 2.

For case 4, the model is subjected to uniformly-distributed load m_0 = 420 KN·m/m over the length of the span. For case 5, the model is subjected to a concentrated load m_0 = 150 KN·m at the mid-span section ($c = {}^1/_2$). Figs. 14-21 show the vertical deflection, torsional angle,

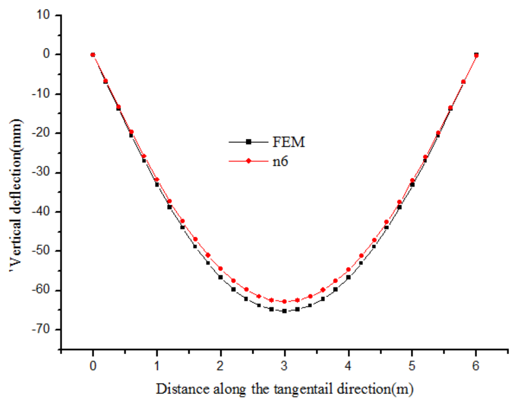

Fig. 14 Vertical deflection of the case 4 with K = 250 MPa

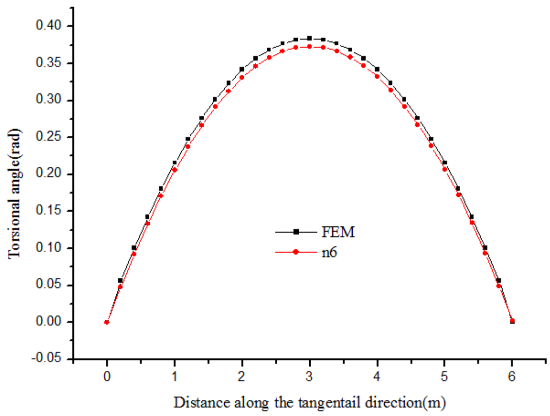

Fig. 15 Torsional angle of the case 4 with K = 250 MPa

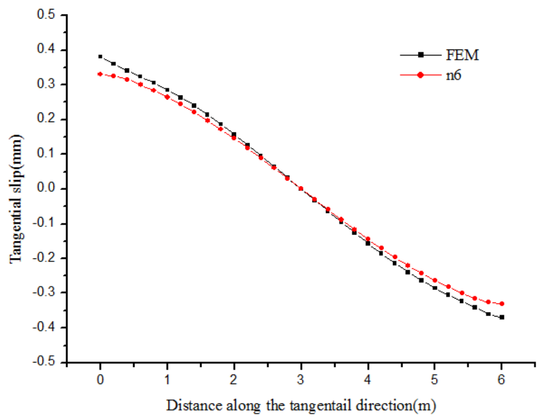

Fig. 16 Tangential slip of the case 4 with K = 250 MPa

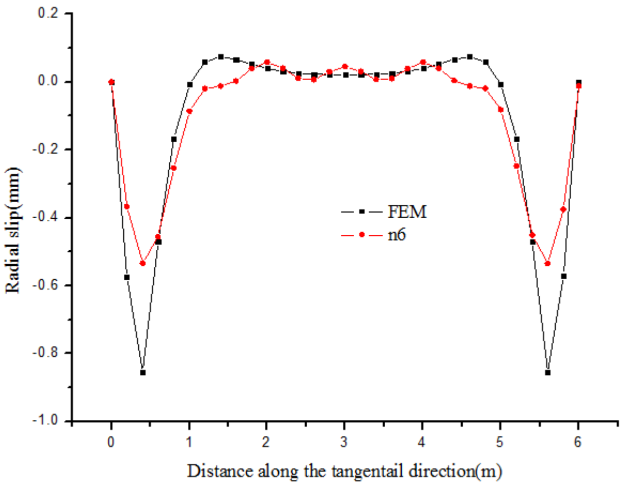

Fig. 17 Radial slip of the case 4 with K = 250 MPa

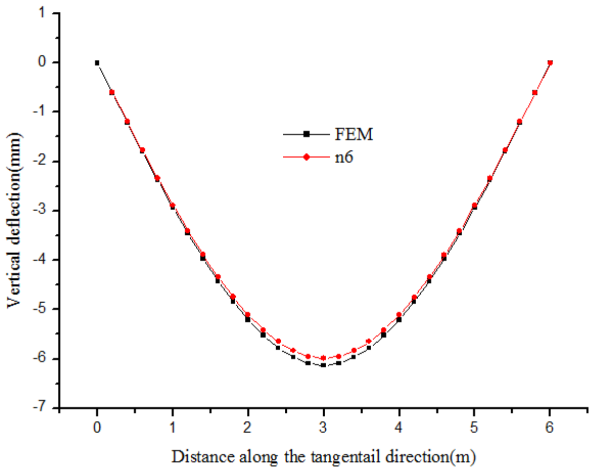

Fig. 18 Vertical deflection of the case 5 with K = 250 MPa

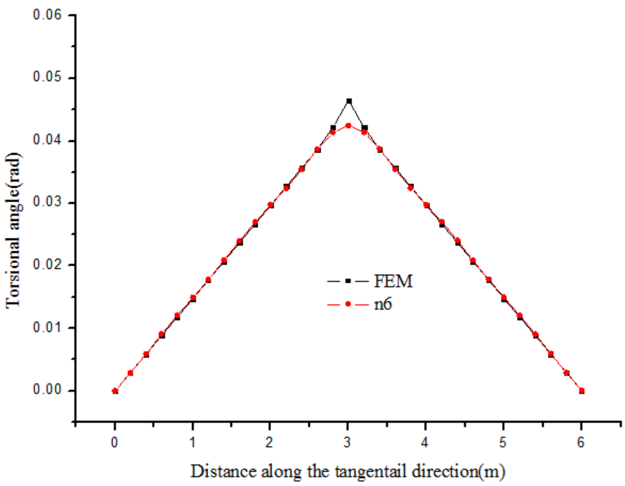

Fig. 19 Torsional angle of the case 5 with K = 250 MPa

tangential slip and radial slip based on the FEM and this paper results, respectively.

In Figs. 14-21, it can be seen that this paper results are in concordance with the results of FEM. Fig. 17 shows the

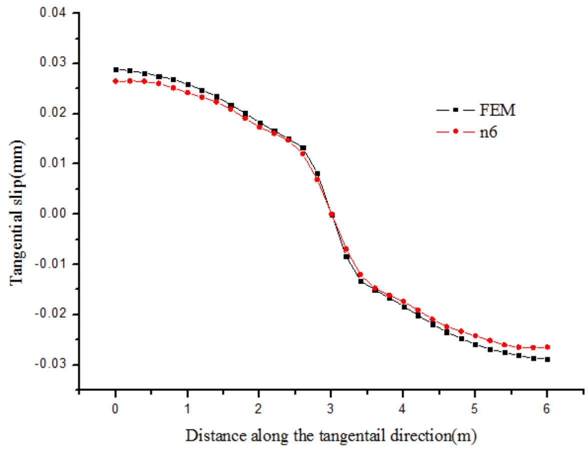

Fig. 20 Tangential slip of the case 5 with K = 250 MPa

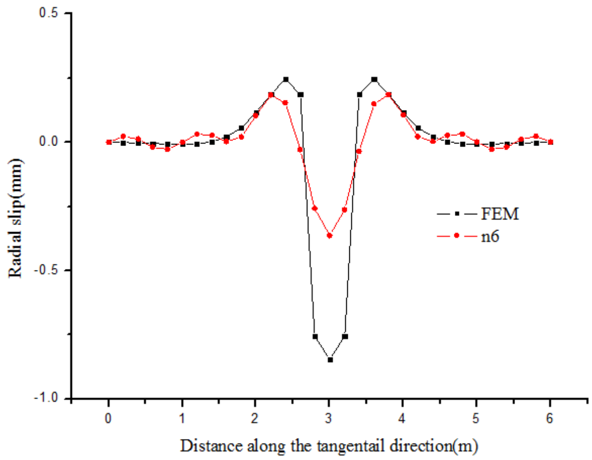

Fig. 21 Radial slip of the case 5 with K = 250 MPa

error of radial slip is bigger at two ends by the comparative analysis between the two methods. The error of torsional angle in Fig. 19 and the error of radial slip in Fig. 21 are bigger between the two methods at midspan section. This shows that the local stress concentration is the cause of the big error between the two methods.

9. Conclusions

In this paper, a semi-analytical solution has been developed and presented for the simply supported composite curved I-beam by trigonometric series. The solution is for a static problem of a two-layered composite curved beam with flexible shear connection. The solution expression use trigonometric functions in terms of span coordinate. Governing equations and boundary conditions are obtained by using the variational approach. The numerical results are compared with other available results in the literature and FEM results. From examples one can see that this method is simpler, effectiveness, easily handled and suitable for practical design work. Thus the model in this paper can be applied sufficiently for practical purposes.

Acknowledgments

The research described in this paper was financially supported by the National Natural Science Foundation of China (51378236) and project supported by the transportation science and technology plan of Jilin province (2016-1-17).

References

Arefi, M. and Zenkour, A.M. (2017), "Electro-magneto-elastic analysis of a three-layer curved beam", *Smart Struct. Syst., Int. J.*, **19**(6), 695-703. DOI: 10.12989/sss.2017.19.6.695

Campi, F. and Monetto, I. (2013), "Analytical solutions of two-layer beams with interlayer slip and bi-linear interface law", *Int. J. Solids Struct.*, **50**(5), 687-698.

Chakrabarti, A., Sheikh, A.H., Griffith, M. and Oehlers, D.J. (2012), "Analysis of composite beams with longitudinal and transverse partial interactions using higher order beam theory", *Int. J. Mech. Sci.*, **59**(1), 115-125.

Dall'Asta, A. (2001), "Composite beams with weak shear connection", *Int. J. Solids Struct.*, **38**(38), 5605-5624.

Erkmen, R.E. and Bradford, M.A. (2009), "Nonlinear elastic analysis of composite beams curved in-plan", *Eng. Struct.*, **31**(7), 1613-1624.

Gimena, L., Gimena, F.N. and Gonzaga, P. (2008), "Structural analysis of a curved beam element defined in global coordinates", *Eng. Struct.*, **30**(11), 3355-3364.

Girhammar, U.A. and Gopu, V.K.A. (1993), "Composite beam-columns with interlayer slip-exact analysis", *J. Struct. Eng. - ASCE*, **199**(4), 1265-1282.

Giussani, F. and Mola, F. (2006), "Service-stage analysis of curved composite steel_concrete bridge beams", *J. Struct. Eng. - ASCE*, **132**(12), 1928-1939.

Kim, N.I. (2009), "Dynamic stiffness matrix of composite box beams", *Steel Compos. Struct., Int. J.*, **9**(5), 473-497.

Kim, M.Y., Kim, S.B. and Kim, N.I. (2005a), "Spatial stability of shear deformable curved beams with non-symmetric thin walled sections, I: Stability formulation and closed form solutions", *Comput. Struct.*, **83**(31-32), 2525-2541.

Kim, M.Y., Kim, S.B. and Kim, N.I. (2005b), "Spatial stability of shear deformable curved beams with non-symmetric thin walled sections, II: F.E. Solutions and parametric study", *Comput. Struct.*, **83**(31-32), 2542-2558.

Liu, H.B., Liu, W.H. and Zhang, Y.L. (2005),"Calculation analysis of shearing slip for steel-concrete composite beam under concentrated load", *Appl. Math. Mech.-Engl. Ed.*, **26**(6), 735-740.

Liu, X., Erkmen, R.E. and Bradford, M.A. (2012), "Creep and shrinkage analysis of curved composite beams with partial interaction", *Int. J. Mech. Sci.*, **58**(1), 57-68.

Liu, H.L., Zhu, X.F. and Yang, D.X. (2016), "Isogeometric method based in-plane and out-of-plane free vibration analysis for Timoshenko curved beams", *Struct. Eng. Mech., Int. J.*, **59**(3), 503-526.

Majdi, Y., Hsu, C.T.T. and Zarei, M. (2014), "Finite element analysis of new composite floors having cold-formed steel and concrete slab", *Eng. Struct.*, **77**(15), 65-83.

Palani, G.S. and Rajesekan, S. (1992), "Finite element analysis of thin-walled curved beams made of composites", *J. Struct. Eng. - ASCE*, **118**(8), 2039-2062.

Pi, Y.L., Bradford, M.A. and Uy, B. (2006), "Second order nonlinear inelastic analysis of composite steel-concrete members. I: Theory", *J. Struct. Eng. - ASCE*, **132**(5), 751-761.

Prokic, A., Lukic, D. and Ladjinovic, D. (2014), "Automatic analysis of thin-walled laminated composite sections", *Steel Compos. Struct., Int. J.*, **16**(3), 233-252.

Qin, X.X., Liu, H.B., Wu, C.L. and Gu, Z.W. (2016), "A trigonometric analytical solution of simply supported horizontally curved composite I-beam considering tangential slips", *Math. Problem. Eng.*, 1-12.

Ranzi, G., Bradford, M.A. and Uy, B. (2003), "A general method of analysis of composite beams with partial interaction", *Steel Compos. Struct., Int. J.*, **3**(3), 169-184.

Santos, H.A.F.A. and Silberschmidt, V.V. (2014), "Hybrid equilibrium finite element formulation for composite beams with partial interaction", *Comput. Struct.*, **108**(1), 646-656.

Tan, E.L. and Uy, B. (2009), "Experimental study on curved composite beams subjected to combined flexure and torsion", *J. Constr. Steel Res.*, **65**(4), 784-793.

Tan, E.L. and Uy, B. (2011), "Nonlinear analysis of composite beams subjected to combined flexure and torsion", *J. Constr. Steel Res.*, **67**(5), 760-799.

Thevendran, V., Chen, S., Shanmugam, N.E. and Liew, J.Y.R. (1999), "Nonlinear analysis of steel-concrete composite beams curved in plan", *Finite Elem. Anal. Des.*, **32**(3), 125-139.

Thevendran, V., Shanmugam, N.E., Chen, S. and Liew, J.Y.R. (2000), "Experimental study on steel_concrete composite beams curved in plan", *Eng. Struct.*, **22**(8), 877-889.

Topkaya, C., Williamson, E.B. and Frank, K.H. (2004), "Behavior of curved steel trapezoidal box-girders during construction", *Eng. Struct.*, **26**(6), 721-733.

Vlasov, V.Z. (1961), Thin walled elastic beams, Israel Program for Scientific Translation, Jerusalem.

Wilson, J.F., Wang, Y. and Threlfall, I. (1999), "Responses of near-optimal, continuous horizontally curved beams to transit loads" *J. Sound Vib.*, **222**(4), 565-575.

Yu, A.M., Yang, J.W., Nie, G.H. and Yang, X.G. (2011), "An improved model for naturally curved and twisted composite beams with closed thin-walled sections", *Comput. Struct.*, **93**(9), 2322-2329.

Yu, A.M., Yang, X.G. and Nie, G.H. (2006), "Generalized coordinate for warping of naturally curved and twisted beams with general cross-sectional shapes", *Int. J. Solids Struct.*, **43**(10), 2853-2867.

Zona, A. and Ranzi, G. (2011), "Finite element models for nonlinear analysis of steel–concrete composite beams with partial interaction in combined bending and shear", *Finite Elem. Anal. Des.*, **47**(2), 98-118.

CC

Appendix A

$$\Gamma_1 = EI_x u_y'''' - GI_T \frac{u_y''}{R^2} - \frac{EI_x + GI_T}{R}\phi_z'' + b\lambda_z'' + \frac{b\lambda_y''}{R} - q_0$$

$$\Gamma_2 = -\frac{EI_x + GI_T}{R} u_y'' - GI_T\phi_z'' + \frac{EI_x}{R^2}\phi_z - \frac{b\lambda_z}{R} + b\lambda_y'' - m_0$$

$$\Gamma_3 = [E_1A_1(u_{1z}' - \frac{u_{1x}}{R})'' + \frac{E_1I_{y1}}{R}(u_{1x}'' + \frac{u_{1z}'}{R})'']\frac{1}{K_t}$$
$$+\frac{1}{RK_r}[E_1I_{y1}(u_{1x}'' + \frac{u_{1z}'}{R})'' - \frac{E_1A_1}{R}(u_{1z}' - \frac{u_{1x}}{R})]$$
$$-S_A E_1A_1(u_{1z}' - \frac{u_{1x}}{R}) + u_y''b - \frac{\phi_z b}{R}$$

$$\Gamma_4 = [E_1A_1(u_{1z}' - \frac{u_{1x}}{R})'' + \frac{E_1I_{y1}}{R}(u_{1x}'' + \frac{u_{1z}'}{R})'']\frac{1}{RK_t}$$
$$-\frac{1}{K_r}[E_1I_{y1}(u_{1x}'' + \frac{u_{1z}'}{R})'''' - \frac{E_1A_1}{R}(u_{1z}' - \frac{u_{1x}}{R})'']$$
$$-S_y E_1I_{y1}(u_{1x}'' + \frac{u_{1z}'}{R}) + \phi_z''b + \frac{u_y''b}{R}$$

$$\Gamma_5 = E_1I_{y1}S_y[E_1I_{y1}(u_{1x}'' + \frac{u_{1z}'}{R}) - \lambda_y]''$$
$$-E_1A_1S_A\frac{1}{R}[E_1A_1(u_{1z}' - \frac{u_{1x}}{R}) - \lambda_z]$$
$$+\frac{E_1A_1}{K_tR}[E_1A_1(u_{1z}' - \frac{u_{1x}}{R})$$
$$+\frac{E_1I_{y1}}{R}(u_{1x}'' + \frac{u_{1z}'}{R}) - \lambda_z - \frac{\lambda_y}{R}]''$$
$$-\frac{E_1I_{y1}}{K_tR}[E_1A_1(u_{1z}' - \frac{u_{1x}}{R})$$
$$+\frac{E_1I_{y1}}{R}(u_{1x}'' + \frac{u_{1z}'}{R}) - \lambda_z - \frac{\lambda_y}{R}]''''$$
$$+\frac{E_1I_{y1}}{K_r}[E_1I_{y1}(u_{1x}'' + \frac{u_{1z}'}{R})''$$
$$-\frac{1}{R}E_1A_1(u_{1z}' - \frac{u_{1x}}{R}) + \frac{\lambda_z}{R} - \lambda_y'']''''$$
$$+\frac{E_1A_1}{R^2K_r}[E_1I_{y1}(u_{1x}'' + \frac{u_{1z}'}{R})''$$
$$-\frac{1}{R}E_1A_1(u_{1z}' - \frac{u_{1x}}{R}) + \frac{\lambda_z}{R} - \lambda_y'']$$

$$\Gamma_6 = \frac{1}{K_t}[E_1A_1(u_{1z}' - \frac{u_{1x}}{R}) + \frac{E_1I_{y1}}{R}(u_{1x}'' + \frac{u_{1z}'}{R})$$
$$-\lambda_z - \frac{\lambda_y}{R}]'''(E_1A_1 + \frac{E_1I_{y1}}{R^2}) - E_1A_1S_A[E_1A_1(u_{1z}' - \frac{u_{1x}}{R}) - \lambda_z]'$$
$$-\frac{S_yE_1I_{y1}}{R}[E_1I_{y1}(u_{1x}'' + \frac{u_{1z}'}{R}) - \lambda_y]'$$
$$-\frac{E_1I_{y1}}{RK_r}[E_1I_{y1}(u_{1x}'' + \frac{u_{1z}'}{R})''$$
$$-\frac{1}{R}E_1A_1(u_{1z}' - \frac{u_{1x}}{R}) + \frac{\lambda_z}{R} - \lambda_y'']'''$$
$$+\frac{E_1A_1}{RK_r}[E_1I_{y1}(u_{1x}'' + \frac{u_{1z}'}{R})''$$
$$-\frac{1}{R}E_1A_1(u_{1z}' - \frac{u_{1x}}{R}) + \frac{\lambda_z}{R} - \lambda_y'']'$$

$$H_1 = -EI_x(u_y''' - \frac{\phi_z'}{R}) - b\lambda_z' - \frac{b}{R}\lambda_y' + GI_T(\frac{\phi_z'}{R} + \frac{u_y'}{R^2}) - Q_{yt}$$

$$H_2 = EI_x(u_y'' - \frac{\phi_z}{R}) + b\lambda_z + \frac{b}{R}\lambda_y - M_{xt}$$

$$H_3 = GI_T(\phi_z' + \frac{u_y'}{R}) - b\lambda_y' - T_{zt}$$

$$H_4 = b\lambda_y$$

$$H_5 = \lambda_z + \frac{\lambda_y}{R}$$

$$H_6 = \lambda_y'$$

$$H_7 = -\lambda_y$$

$$H_8 = E_1A_1S_A[E_1A_1(u_{1z}' - \frac{u_{1x}}{R}) - \lambda_z]$$
$$+\frac{S_yE_1I_{y1}}{R}[E_1I_{y1}(u_{1x}'' + \frac{u_{1z}'}{R}) - \lambda_y]$$
$$-\frac{1}{K}[E_1A_1(u_{1z}' - \frac{u_{1x}}{R}) + \frac{E_1I_{y1}}{R}(u_{1x}'' + \frac{u_{1z}'}{R})$$
$$-\lambda_z - \frac{\lambda_y}{R}]''(E_1A_1 + \frac{E_1I_{y1}}{R^2})$$
$$+\frac{E_1I_{y1}}{RK_r}[E_1I_{y1}(u_{1x}'' + \frac{u_{1z}'}{R})''$$
$$-\frac{E_1A_1}{R}(u_{1z}' - \frac{u_{1x}}{R}) + \frac{\lambda_z}{R} - \lambda_y'']''$$
$$-\frac{E_1A_1}{RK_r}[E_1I_{y1}(u_{1x}'' + \frac{u_{1z}'}{R})''$$
$$-\frac{E_1A_1}{R}(u_{1z}' - \frac{u_{1x}}{R}) + \frac{\lambda_z}{R} - \lambda_y'']$$

$$H_9 = \frac{1}{K_t}[E_1A_1(u_{1z}{}' - \frac{u_{1x}}{R}) + \frac{E_1I_{y1}}{R}(u_{1x}{}'' + \frac{u_{1z}{}'}{R})$$
$$-\lambda_z - \frac{\lambda_y}{R}]'(E_1A_1 + \frac{E_1I_{y1}}{R^2})$$
$$-\frac{E_1I_{y1}}{RK_r}[E_1I_{y1}(u_{1x}{}'' + \frac{u_{1z}{}'}{R})''$$
$$-\frac{E_1A_1}{R}(u_{1z}{}' - \frac{u_{1x}}{R}) + \frac{\lambda_z}{R} - \lambda_y{}'']'$$

$$H_{10} = \frac{E_1I_{y1}}{RK_r}[E_1I_{y1}(u_{1x}{}'' + \frac{u_{1z}{}'}{R})''$$
$$-\frac{E_1A_1}{R}(u_{1z}{}' - \frac{u_{1x}}{R}) + \frac{\lambda_z}{R} - \lambda_y{}'']$$

$$H_{11} = -E_1I_{y1}S_y[E_1I_{y1}(u_{1x}{}'' + \frac{u_{1z}{}'}{R}) - \lambda_y]'$$
$$-\frac{E_1A_1}{K_tR}[E_1A_1(u_{1z}{}' - \frac{u_{1x}}{R})'$$
$$+\frac{E_1I_{y1}}{R}(u_{1x}{}'' + \frac{u_{1z}{}'}{R})' - \lambda_z{}' - \frac{\lambda_y{}'}{R}]$$
$$+\frac{E_1I_{y1}}{K_tR}[E_1A_1(u_{1z}{}' - \frac{u_{1x}}{R})'$$
$$+\frac{E_1I_{y1}}{R}(u_{1x}{}'' + \frac{u_{1z}{}'}{R})' - \lambda_z{}' - \frac{\lambda_y{}'}{R}]''$$
$$-\frac{E_1I_{y1}}{K_r}[E_1I_{y1}(u_{1x}{}'' + \frac{u_{1z}{}'}{R})''$$
$$-\frac{E_1A_1}{R}(u_{1z}{}' - \frac{u_{1x}}{R}) + \frac{\lambda_z}{R} - \lambda_y{}'']'''$$

$$H_{12} = E_1I_{y1}S_y[E_1I_{y1}(u_{1x}{}'' + \frac{u_{1z}{}'}{R}) - \lambda_y]$$
$$-\frac{E_1I_{y1}}{K_tR}[E_1A_1(u_{1z}{}' - \frac{u_{1x}}{R})'$$
$$+\frac{E_1I_{y1}}{R}(u_{1x}{}'' + \frac{u_{1z}{}'}{R})' - \lambda_z{}' - \frac{\lambda_y{}'}{R}]'$$
$$+\frac{E_1I_{y1}}{K_r}[E_1I_{y1}(u_{1x}{}'' + \frac{u_{1z}{}'}{R})''$$
$$-\frac{E_1A_1}{R}(u_{1z}{}' - \frac{u_{1x}}{R}) + \frac{\lambda_z}{R} - \lambda_y{}'']''$$

$$H_{13} = \frac{E_1I_{y1}}{K_tR}[E_1A_1(u_{1z}{}' - \frac{u_{1x}}{R})'$$
$$+\frac{E_1I_{y1}}{R}(u_{1x}{}'' + \frac{u_{1z}{}'}{R})' - \lambda_z{}' - \frac{\lambda_y{}'}{R}]$$
$$-\frac{E_1I_{y1}}{K_r}[E_1I_{y1}(u_{1x}{}'' + \frac{u_{1z}{}'}{R})''$$
$$-\frac{E_1A_1}{R}(u_{1z}{}' - \frac{u_{1x}}{R}) + \frac{\lambda_z}{R} - \lambda_y{}'']'$$

$$H_{14} = \frac{E_1I_{y1}}{K_r}[E_1I_{y1}(u_{1x}{}'' + \frac{u_{1z}{}'}{R})''$$
$$-\frac{E_1A_1}{R}(u_{1z}{}' - \frac{u_{1x}}{R}) + \frac{\lambda_z}{R} - \lambda_y{}'']$$